MINERALOGICAL MAGAZINE

VOLUME 61 NUMBER 406 JUNE 1997

Cognate gabbroic xenoliths from a tholeiitic subvolcanic sill complex: Implications for fractional crystallization and crustal contamination processes

R. J. PRESTON[1,2] AND B. R. BELL

Department of Geology and Applied Geology, University of Glasgow, Glasgow, G12 8QQ, UK

Abstract

Intruded into the Palaeogene lava field and underlying Moine (Neoproterozoic) crystalline basement rocks around Loch Scridain, Isle of Mull, Scotland, is a suite of high-level, inclined, xenolithic sheets, ranging in composition from basalt, through andesite and dacite, to rhyolite. These sheets, associated with the Mull central volcano, were emplaced post 55 Ma. As well as numerous crustal xenoliths, the more basic members of the complex contain a diverse suite of ultrabasic and basic xenoliths. Xenolith types include feldspathic peridotite with cumulus olivine, pyroxenite, gabbro with cumulus plagioclase and cumulus clinopyroxene, and pure anorthosite. Mineralogical data, coupled with whole-rock major- and trace-element data from a small number of the xenoliths suggest that the xenoliths represent early-formed cumulates cognate with their host basalts. Sr and Nd isotope data from the xenoliths confirms the cognate origin, and also shows that the basic magmas suffered crustal contamination at an early stage.

KEYWORDS: xenolith, feldspathic peridotite, pyroxenite, gabbro, anorthosite, fractional crystallization, crustal contamination.

Introduction

THE presence of 'non-mantle'-derived ultramafic and mafic xenoliths in suites of volcanic and hypabyssal rocks is widely reported (e.g. Arculus and Wills, 1980; Harris, 1983; Munha *et al.*, 1990). They appear to be common in island-arc calc-alkaline/alkaline suites (e.g. DeLong *et al.*, 1975; Cigolini and Kudo, 1987), and in continental and oceanic alkaline rocks (e.g. Binns *et al.*, 1970). Certain occurrences are thought to be related to the host magmas via a process of earlier high-pressure crystal fractionation (e.g. Binns, 1969). Such xenoliths are reported less

[1] Present address: Department of Geology and Petroleum Geology, Meston Building, King's College, University of Aberdeen, Old Aberdeen, AB24 3UE. Telephone: (01224) 273467
e:mail: j.preston@abdn.ac.uk

[2] SURRC contact: Dr G. Rogers - Isotope Geosciences Unit, Scottish Universities Research & Reactor Centre, East Kilbride, Glasgow, G75 0QF, UK.

Mineralogical Magazine, June 1997, Vol. 61, pp. 329–349

frequently from continental tholeiitic suites. However, examples have been reported from the British Tertiary Igneous Province (BTIP). Donaldson (1977) described olivine-anorthite, augite-anorthite, olivine-labradorite, and anorthite cumulate xenoliths from gabbroic anorthosite dykes, of tholeiitic affinity, from north-west Skye, and Gibb (1969) described dunitic and peridotitic xenoliths from ultrabasic dykes in central Skye. These occurrences are considered to represent fragments of early-formed cognate cumulates (Gibb, 1969; Donaldson, 1977).

The present study concentrates on a suite of high-level subvolcanic conduits which intrude the Palaeogene lavas and older rocks around the shores of Loch Scridain, Isle of Mull, NW Scotland (Fig.1). The Loch Scridain Sill Complex (LSSC) consists of fine-grained tholeiitic basalts and basaltic andesites, tholeiitic andesites, porphyritic dacites and a smaller number of rhyolites (Bailey *et al.*, 1924; Preston, 1996). The basic sheets are markedly xenolithic, containing numerous silicic and aluminous crustal xenoliths, along with a smaller number of ultramafic and gabbroic xenoliths. It is the ultramafic and gabbroic xenoliths which form the basis for this study, which uses mineralogical and textural data, along with mineral chemistry and whole-rock bulk geochemistry, to constrain their origin and petrogenesis.

Analytical techniques

All mineral analyses were carried out on the Cameca SX-50 electron probe microanalyser fitted with four wavelength spectrometers at the Department of Geology and Applied Geology, University of Glasgow. Typical working conditions were 15 kV and 20 nA, with a beam size of between 1–3 μm. Standards comprised a series of pure elements and compounds supplied by Cameca and Micro analysis Consultants Ltd.

Whole-rock major- and trace-element analyses were carried out using a Philips PW 1480 automatic X-ray fluorescence spectrometer in the Department of Geology and Geophysics, University of

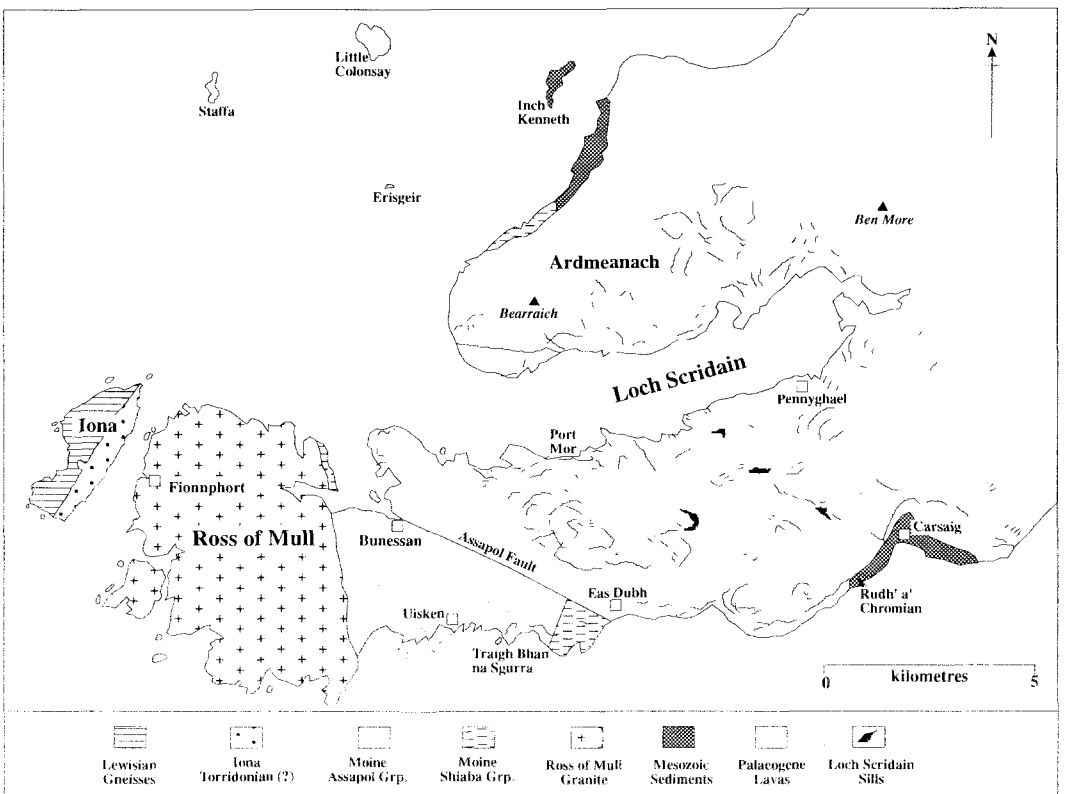

FIG. 1. Sketch map showing general geology of the Ross of Mull and Loch Scridain area. Number of sheets shown in LSSC greatly reduced for clarity.

Edinburgh. Sample preparation, and accuracy and precision of the analyses have been described by Fitton and Dunlop (1985). Whole-rock *REE* analyses were performed at the Department of Geology, Royal Holloway University, London, by inductively coupled plasma atomic emission spectroscopy (ICP-AES). Details of the ion-exchange separation technique of the *REE* from whole-rock samples, together with running procedures, accuracy, and precision of the ICP-AES have been described by Walsh *et al.* (1981).

Rb-Sr and Sm-Nd isotopic data were determined at the Scottish Universities Research and Reactor Centre (SURRC), East Kilbride. Details of the separation techniques have been reported by Janošek *et al.* (1995), and by Barbero *et al.* (1995). Sr, Nd and Sm isotope analyses were performed on a VG Sector 54-30 thermal ionisation mass spectrometer, whereas Rb analyses were carried out using a VG MM30 thermal ionisation mass spectrometer. During the course of this study, the JM Nd standard gave $^{143}Nd/^{144}Nd = 0.511500 \pm 10$ (2s.d), and repeat analyses of NBS 987 Sr standard gave $^{87}Sr/^{86}Sr = 0.710236 \pm 19$ (2s.d.).

Occurrence, field characteristics and mineralogy

The gabbroic xenoliths were briefly described by Bailey *et al.* (1924), and were considered to be cognate in origin, although no detailed reasoning was put forward. The xenoliths are generally found near the base of the sheets, suggesting that they were denser than the host magma and the associated aluminous xenoliths, the latter tending to be found near the top surfaces of the sheets (Preston, 1996). The xenoliths vary in size from single crystals (xenocrysts) and crystal aggregates a few cm across, to large rounded blocks up to a metre in diameter. Mineralogically, they consist of a combination of olivine, pyroxene and plagioclase. All xenolith types are medium- to coarse-grained plutonic rocks, none of which exhibit igneous layering or possess a tectonic fabric. Their coarse-grained and often near-monomineralic nature suggests that they formed through the accumulation of primocrysts, by whatever mechanism, and are therefore considered to be cumulates in the broadest sense (e.g. McBirney and Hunter, 1995).

Four distinct ultramafic-mafic xenolith types have been found within the LSSC:

(a) Feldspathic peridotite: 55–64% cumulus olivine, 20–28% cumulus plagioclase, 5–10% intercumulus pyroxene, 5–8% fine-grained intercumulus plagioclase and pyroxene;

(b) Pyroxenite: 58–63% cumulus pyroxene, 32–40% intercumulus plagioclase, 2–5% Fe–Ti oxides;

(c) Gabbro: 37–42% cumulus or intercumulus pyroxene, 51–60% cumulus plagioclase, 3–7% fine-grained intercumulus plagioclase and pyroxene;

(d) Anorthosite: 95–98% cumulus plagioclase, 2–5% fine-grained intercumulus plagioclase and pyroxene.

Olivine-plagioclase cumulate (feldspathic peridotite)

These are the most common cumulate xenoliths found (~50%). They are generally the largest type, and consist of dark green or black, rounded blocks up to 1 metre in diameter. The blocks are often highly friable, presumably due to pervasive alteration. In thin-section they consist of cumulus olivine (mode ~ 60%), which forms round to subhedral grains up to 5 mm in diameter (Fig 2.). Alteration to serpentine and red-brown iddingsite is ubiquitous along cracks and around crystal margins. Some crystals are completely pseudomorphed by serpentine, in places accompanied by aggregates of tiny magnetite crystals. However, much of the olivine is fresh, and compositions range from Fo_{80} to Fo_{83}. Some olivines contain inclusions of chrome-spinel, which forms euhedral crystals a few μm across, and which are homogeneous in composition. Cr-spinel also occurs in embayments within individual olivine crystals, and also disseminated through the intercumulus clinopyroxene and cumulus plagioclase. There is some inter-sample variation in Cr-spinel composition: $(Mg_{0.58}Fe^{2+}_{0.42})(Cr_{0.85}Al_{0.90}Fe^{3+}_{0.21})O_4$ to $(Mg_{0.54}Fe^{2+}_{0.46})(Cr_{1.10}Al_{0.65}Fe^{3+}_{0.25})O_4$. This variation appears to be related to the nature of the individual crystal's immediate environment. Those Cr-spinels trapped in cumulus olivine tend to be the most Mg and Al-rich, whereas those contained within plagioclase or

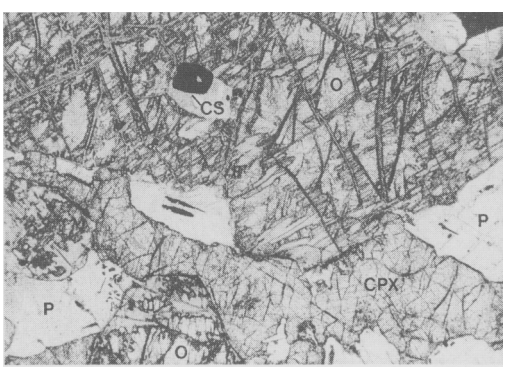

FIG. 2. Photomicrograph of a feldspathic peridotite, showing cumulus olivine (O) with inclusions of Cr-spinel (CS), with poikilitic clinopyroxene (CPX) and minor intercumulus plagioclase (P). Field of view 2 × 3 mm.

clinopyroxene are the most Cr-rich. The chrome-spinel is considered to be an early cumulus phase. There is also minor cumulus plagioclase, which forms laths up to 3 mm in length. The plagioclase generally has complex twinning and is invariably strongly zoned ($An_{87} - An_{67}$), core to rim. There does not appear to be any adcumulate growth of either the olivine or the plagioclase, although the zoned nature of the plagioclase crystals might warrant these rocks being described as mesocumulates (*cf.* Conrad and Kay, 1984).

Clinopyroxene occurs as intercumulus crystals. It is generally fresh, and is a pale-brown, non-pleochroic variety. Individual crystals show no zoning, but there is slight compositional variation within each sample, from $Wo_{41}En_{49}Fs_{10}$ to $Wo_{45}En_{45}Fs_{10}$. Intercumulus plagioclase is also present and has the same composition as the cumulus feldspar. A small amount ($\sim$5%) of intercumulus liquid has quenched to a fine-grained mixture of plagioclase (An_{45}), diopsidic-augite ($Wo_{45}En_{45}Fs_{10}$) and magnetite. Those cumulus plagioclase crystals which project into these fine-grained areas tend to have well-formed crystal edges, and often have an overgrowth rim similar in composition to the fine-grained plagioclase (*cf.* Arculus and Wills, 1980).

Clinopyroxene cumulate (pyroxenite)

This rare variety of xenolith (only one specimen has been found), is pale brown and generally appears fresher than the olivine-plagioclase cumulates. It is dominated by fresh clinopyroxene in thin-section (Fig. 3), which forms large, euhedral grains up to 4 mm across, elongate grains 5 mm long, and, more commonly, round and anhedral grains a few mm across. The cumulus pyroxene is generally strongly zoned, showing marked Fe-enrichment from core to rim ($Wo_{50}En_{41}Fs_9$–$Wo_{36}En_{32}Fs_{32}$). This zoning is not always evident optically. In places there is evidence for a small amount of adcumulate growth of the cumulus pyroxene. Plagioclase is interstitial to the clinopyroxene, forms small (1–2 mm), well-shaped laths, and typically shows continuous normal zoning ($An_{63} - An_{47}$).

Plagioclase-clinopyroxene cumulate (gabbro)

These xenoliths are light-coloured, feldspar-rich rocks, which also contain bright green crystals of pyroxene visible in hand-specimen. In thin-section, the main cumulus phase can be seen to be plagioclase, which forms elongate laths up to 3 mm in length. These crystals are zoned from An_{86} to An_{80}, core to rim, although most show a narrow adcumulate overgrowth at $\sim An_{63}$ (Fig. 4). Clinopyroxene has crystallized either as a cumulus phase, forming large (3–4 mm) euhedral crystals, or as an intercumulus phase, often forming large poikilitic plates which partly enclose the cumulus plagioclase (Fig. 5). The clinopyroxene is a diopsidic augite ($Wo_{45}En_{47}Fs_8$), and shows no compositional zoning. As with the other varieties of gabbroic xenolith, approximately 5% of the intercumulus liquid has quenched to a fine-grained mixture of plagioclase (An_{57}), augite ($Wo_{45}En_{45}Fs_{10}$), and titanomagnetite.

Plagioclase cumulate (anorthosite)

One specimen of an extreme plagioclase adcumulate has been found. It is pale grey, and consists almost entirely of feldspar. In thin-section the rock consists

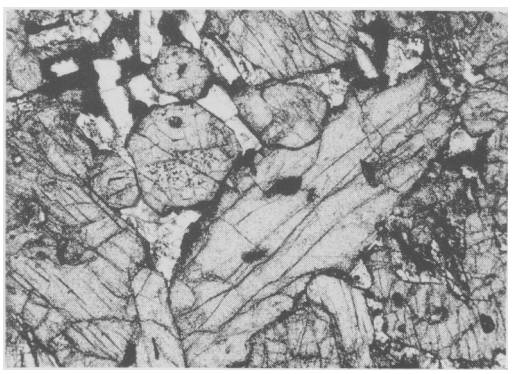

FIG. 3. Photomicrograph of a clinopyroxene cumulate, showing cumulus clinopyroxene and minor intercumulus plagioclase. Field of view 2 × 3 mm.

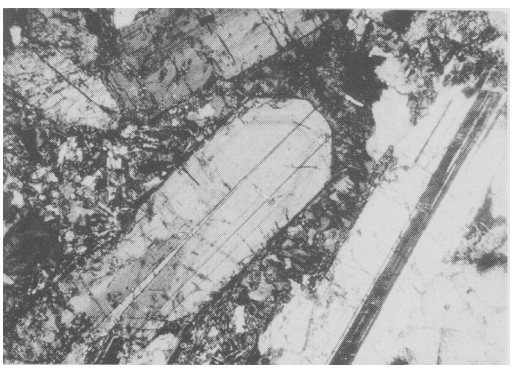

FIG. 4. Photomicrograph of a gabbro, showing zoned cumulus plagioclase and interstitial fine-grained plagioclase and clinopyroxene. Field of view 2 × 3 mm.

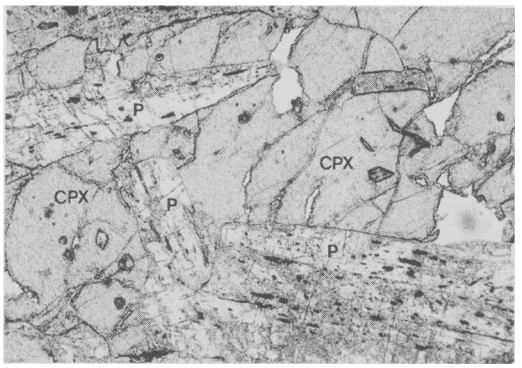

FIG. 5. Photomicrograph of a gabbro, showing large plates of poikilitic clinopyroxene (CPX) enclosing cumulus plagioclase (P). Field of view 2 × 3 mm.

of coarse-grained plagioclase (up to 10 mm) which forms euhedral laths and anhedral grains (Fig. 6). All the grains are interlocking, and there is very little intercumulus material. Each plagioclase crystal in the cumulate rock has distinct normal zoning ($An_{85}-An_{72}$). The plagioclase is extensively fractured, with zeolite occupying fractures. Larger cavities are also filled with radiating clusters of fibrous zeolite. The fracturing may have been due to compaction of the cumulate pile, an interpretation reinforced by the lack of intercumulus material. Alternatively, the passage of hydrothermal fluids, either within the cumulus pile, or after the xenolith had been emplaced within the sheet, may have in itself caused fracturing of the plagioclase.

Mineral chemistry

Mineral compositions of cumulus, intercumulus and quench phases were investigated using electron-probe micro-analysis. The aim was to document

TABLE 1. Representative electron probe micro-analyses of cumulus olivine from a feldspathic peridotite

Sample: Cognate xenolith - KBGX1 (feldspathic peridotite) - cumulus olivine							
Analysis no.	Olivine 1	Olivine 2	Olivine 3 core	Olivine 3 rim	Olivine 4	Olivine 5	Olivine 6
SiO_2	39.43	39.61	39.35	39.35	39.35	39.22	39.58
TiO_2	0.03	0.08	0.05	0.00	0.00	0.12	0.00
Al_2O_3	0.05	0.02	0.05	0.02	0.04	0.05	0.05
Cr_2O_3	0.04	0.04	0.03	0.03	0.05	0.01	0.03
MgO	44.40	44.38	44.57	44.38	44.12	44.90	44.68
CaO	0.26	0.26	0.29	0.29	0.28	0.27	0.22
MnO	0.18	0.24	0.23	0.24	0.23	0.21	0.26
FeO	15.71	15.70	14.82	14.71	14.29	14.48	14.62
NiO	0.09	0.25	0.18	0.19	0.17	0.17	0.07
Total	100.18	100.58	99.58	99.20	98.53	99.43	99.50
Formula based on 4 oxygens							
Si	0.99	0.99	0.99	1.00	1.00	0.99	1.00
Ti	0.00	0.00	0.00	0.00	0.00	0.00	0.00
Al	0.00	0.00	0.00	0.00	0.00	0.00	0.00
Cr	0.00	0.00	0.00	0.00	0.00	0.00	0.00
Mg	1.67	1.66	1.68	1.68	1.67	1.69	1.68
Ca	0.01	0.01	0.01	0.01	0.01	0.01	0.01
Mn	0.00	0.01	0.01	0.01	0.01	0.01	0.01
Fe(ii)	0.33	0.33	0.31	0.31	0.30	0.31	0.31
Ni	0.00	0.01	0.00	0.00	0.00	0.00	0.00
Total	3.01	3.00	3.00	3.00	3.00	3.01	3.00
End-member %							
Fo	83.15	83.15	83.95	83.99	84.30	84.37	84.24
Fa	16.51	15.50	15.66	15.61	15.32	15.26	15.47
Mo	0.34	0.35	0.39	0.40	0.38	0.37	0.29

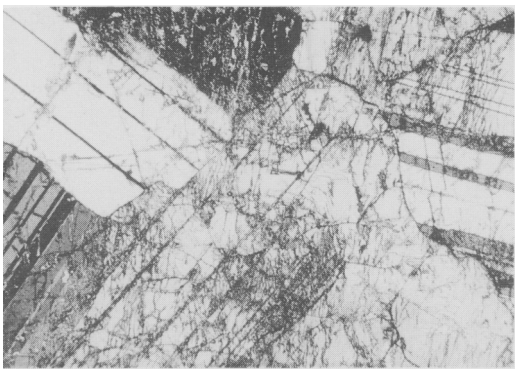

FIG. 6. Photomicrograph of an anorthosite, with slightly zoned cumulus plagioclase showing alteration to zeolite along fractures. Field of view 2 × 3 mm.

inter-sample variations, and to discover the nature of the compositional zonation evident in many of the phases. Representative analyses of each phase from each xenolith type are presented in Tables 1–4.

Olivine

Olivine compositions cover a limited range, varying from Fo_{83} to Fo_{85} (Table 1). Individual crystals show no zoning from core to rim, with compositions generally varying by less than 0.5% Fo. Nickel concentrations are highly variable within any one specimen, and range from 690 ppm to 1980 ppm. There is no correlation between Ni content and olivine composition (*cf.* Donaldson, 1977; Conrad and Kay, 1984; Claydon, 1990). Calcium contents are also variable, ranging from ~1500ppm to 2100ppm. These are generally higher than the calcium contents

TABLE 2. Representative electron probe micro-analyses of cumulus, intercumulus and fine-grained clinopyroxene from the ultramafic and gabbroic xenoliths. All iron determined as FeO* and subsequently partitioned between ferrous and ferric iron by the method of Finger (1972)

Sample	Feldspathic peridotite KBGX1		Pyroxenite KBGX2		Gabbro KBHYX1	
Analysis No.	Interstitial	Fine grained	Cumulus core	Cumulus rim	Cumulus	Fine grained
SiO_2	51.35	49.81	49.53	49.16	52.35	50.15
TiO_2	0.39	0.83	0.66	0.72	0.28	0.85
Al_2O_3	3.47	4.36	4.31	1.76	2.19	3.06
Cr_2O_3	0.58	0.24	0.00	0.01	0.06	0.03
Fe_2O_3	0.38	2.58	3.12	2.60	1.35	2.12
MgO	16.35	14.77	13.66	10.34	16.32	13.65
CaO	20.00	20.42	22.98	16.60	21.80	17.63
FeO	5.75	6.16	4.87	18.21	4.95	12.35
Na_2O	0.26	0.35	0.25	0.30	0.19	0.30
K_2O	0.01	0.01	0.00	0.04	0.01	0.03
Total	98.55	99.53	99.40	99.74	99.49	100.17
Formula based on 6 oxygens						
Si	1.91	1.85	1.85	1.91	1.93	1.89
Al	0.09	0.15	0.15	0.08	0.07	0.11
Al	0.06	0.05	0.04	0.00	0.03	0.03
Fe(iii)	0.01	0.07	0.09	0.08	0.04	0.06
Fe(ii)	0.18	0.19	0.15	0.59	0.15	0.39
Ti	0.01	0.02	0.02	0.02	0.01	0.02
Ca	0.80	0.82	0.92	0.69	0.86	0.71
Mg	0.91	0.82	0.76	0.60	0.90	0.77
Cr	0.02	0.01	0.00	0.00	0.00	0.00
Na	0.02	0.03	0.02	0.02	0.01	0.02
K	0.00	0.00	0.00	0.01	0.00	0.00
Total	4.00	4.00	4.00	4.01	4.00	4.00
End-member %						
Wo	42.34	44.61	50.20	36.72	45.08	38.11
En	48.16	44.89	41.51	31.83	46.94	41.05
Fs	9.5	10.5	8.29	31.44	7.98	20.84

of olivines from the Rum intrusion (Donaldson, 1977) and are more typical of the olivine phenocrysts from the Skye Preshal More olivine tholeiites (Esson *et al.*, 1975). Again, there is no correlation between Ca content and olivine composition (*cf.* Donaldson, 1977). The lack of correlations between the forsterite content and Ni or Ca within the olivines may suggest that they have suffered extensive post-crystallization re-equilibration (e.g. Evans and Moore, 1968).

Clinopyroxene

Clinopyroxene is a major constituent of all the cumulate xenolith types, either as a cumulus or intercumulus phase. The range of clinopyroxene compositions recorded is large, ranging from diopside and salite, through diopsidic-augite, augite, to ferroaugite (Fig. 7). Representative electron-probe micro-analyses of cumulus and intercumulus pyroxenes are given in Table 2. The compositions parallel the trend defined by the pyroxenes of the Skaergaard intrusion (Brown, 1957, Brown and Vincent, 1963; Wager and Brown, 1968). This range in compositions is seen not only within the suite of xenolith types, but also within individual cumulate crystals (Fig. 7). This zonation is extreme, showing a similar iron enrichment to the pyroxenes of the Layered Series of the Skaergaard intrusion (Brown, 1957; Wager and Brown, 1968). No clinopyroxenes examined possessed exsolution laminae of low-Ca pyroxene.

The majority of the clinopyroxenes contain an excess of aluminium after allocation of Al to the tetrahedral site (Fig. 8*a*). The highest Al contents occur in the iron-rich rims of certain cumulus pyroxenes.

Titanium contents vary from 0.005 to 0.024 CPFU, and are, for the most part, positively correlated with Mg# (Fig. 8*b*). The intercumulus clinopyroxenes

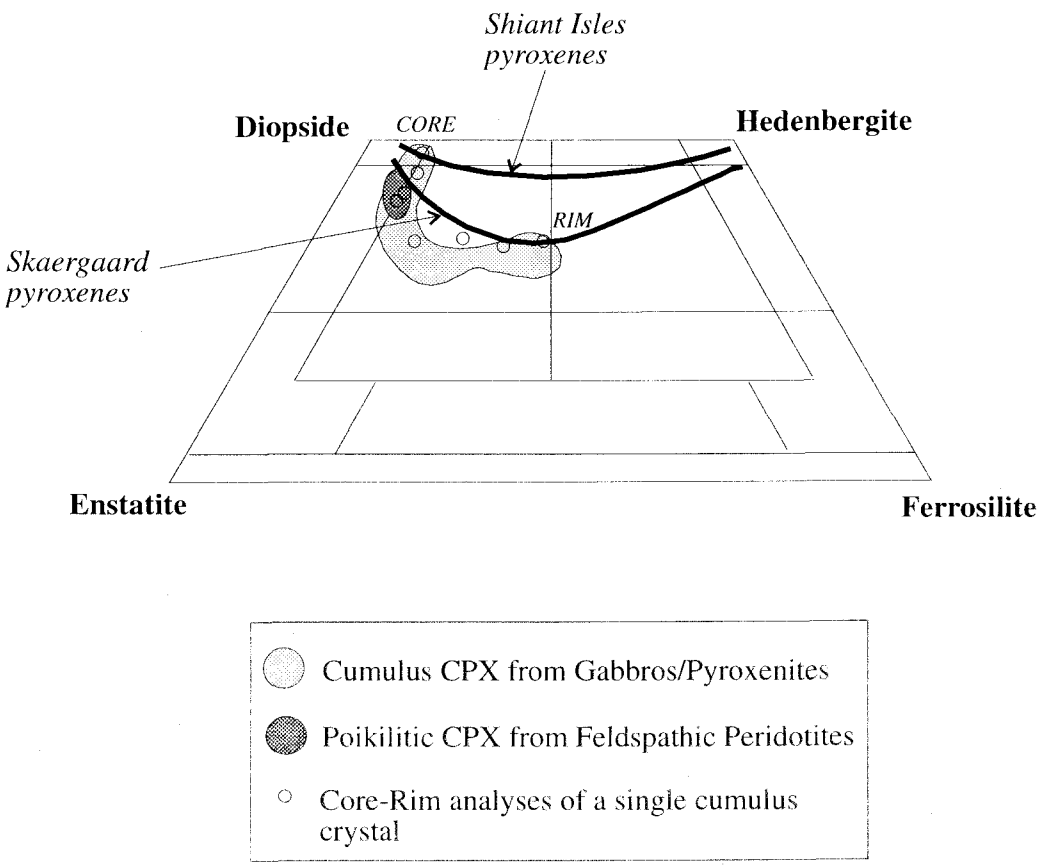

FIG. 7. Clinopyroxene compositions plotted in the pyroxene quadrilateral. Trend for pyroxenes from Skaergaard intrusion from Brown (1957); trend for pyroxenes from the Shiant Isles from Gibb (1973).

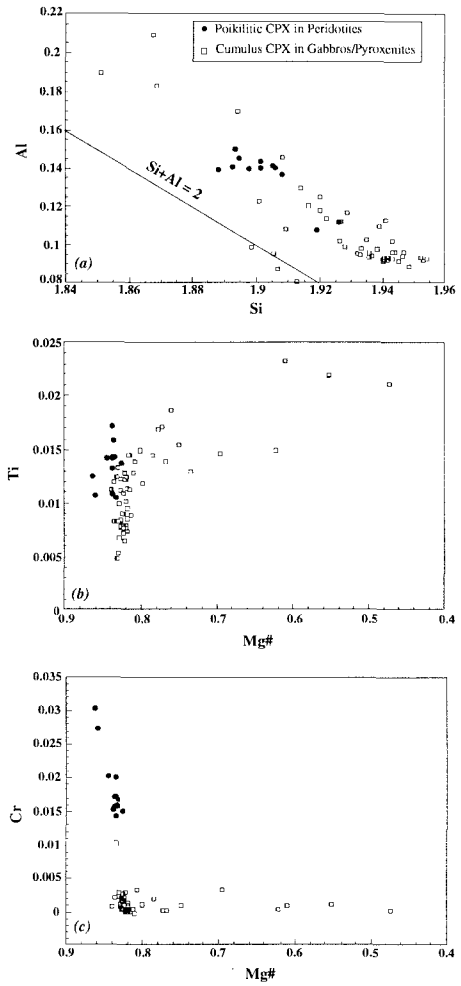

FIG. 8*a-c*. Cation variations in cumulus and intercumulus clinopyroxenes. Cations calculated on the basis of 6 oxygens per formula unit.

from the feldspathic peridotites are, however, more-enriched in Ti. The iron-rich rims to some of the cumulus clinopyroxenes (Mg# 0.76–0.44), although having high Ti contents (0.015–0.024 CPFU) show a decrease in the rate of Ti enrichment with degree of Mg-fractionation (Fig. 8*b*). Titanium shows a positive relationship with total Al content, and a negative correlation with Si (not shown; Preston, 1996).

These relationships between Al, Ti and Si are similar to those seen in the groundmass clinopyroxenes from the host magmas (Preston, 1996). The Al content of calcic-pyroxene is a reflection of the silica activity of the magma (Brown, 1957), and the conditions under which the pyroxene crystallized (Binns *et al.*, 1970), with high Al (and Ti) contents being associated with low Si activities and elevated pressures. As such, the relationships shown are what would be expected in pyroxenes from early-formed cumulates, precipitated at relatively low pressures. The Ti correlations confirm that neither magnetite nor ilmenite were liquidus phases.

Chromium shows a strongly bi-modal correlation with degree of fractionation (Fig. 8*c*). The poikilitic pyroxenes within the peridotites have the highest Cr contents at between 0.013 and 0.028 CPFU, at relatively constant Mg# (0.82–0.86). The cumulus pyroxenes from the gabbros and the pyroxenite have Cr contents generally below 0.005 CPFU. The Cr content remains at this low value with decreasing Mg#. The very steep positive correlation between Cr and Mg# for the feldspathic peridotites suggests that Cr decreased rapidly during magma evolution, presumably due to the early precipitation of Cr-spinel. This confirms that the peridotites were some of the earliest cumulates to form. By the time clinopyroxene became a cumulus phase within the gabbros, the magma had been effectively depleted in Cr.

The intercumulus pyroxenes associated with the feldspathic peridotites are also the least evolved of all those analysed, having an Mg# of 0.82–0.86. This is unusual, in that the cumulus pyroxenes should have the highest Mg#, since these most likely represent near-liquidus compositions (some cumulus pyroxenes do have Mg# at 0.83). Using the equations of Duke (1976), which can be used to calculate the Fe-Mg ratios of mafic melts in equilibrium with olivine and Ca-clinopyroxene, it can be shown that the intercumulus pyroxenes apparently crystallized from a more magnesian liquid than the coexisting cumulus olivine.

Similar observations have been made on peridotites from the lower part of the Eastern Layered Series of the Rum intrusion (Faithfull, 1985). However, it has been suggested that migration of intercumulus liquids in the cumulus pile can cause re-equilibration of certain minerals, particularly olivine and chrome-spinel (Faithfull, 1985; Tait, 1985; Palacz and Tait, 1985; Claydon and Bell, 1992). Faithfull (1985) suggested that such melt movements may be responsible for the anomalous clinopyroxene compositions, although sub-solidus re-equilibration between olivine and clinopyroxene may also be an important process.

Plagioclase

Plagioclase compositions are shown in Fig. 9, and representative analyses are given in Table 3.

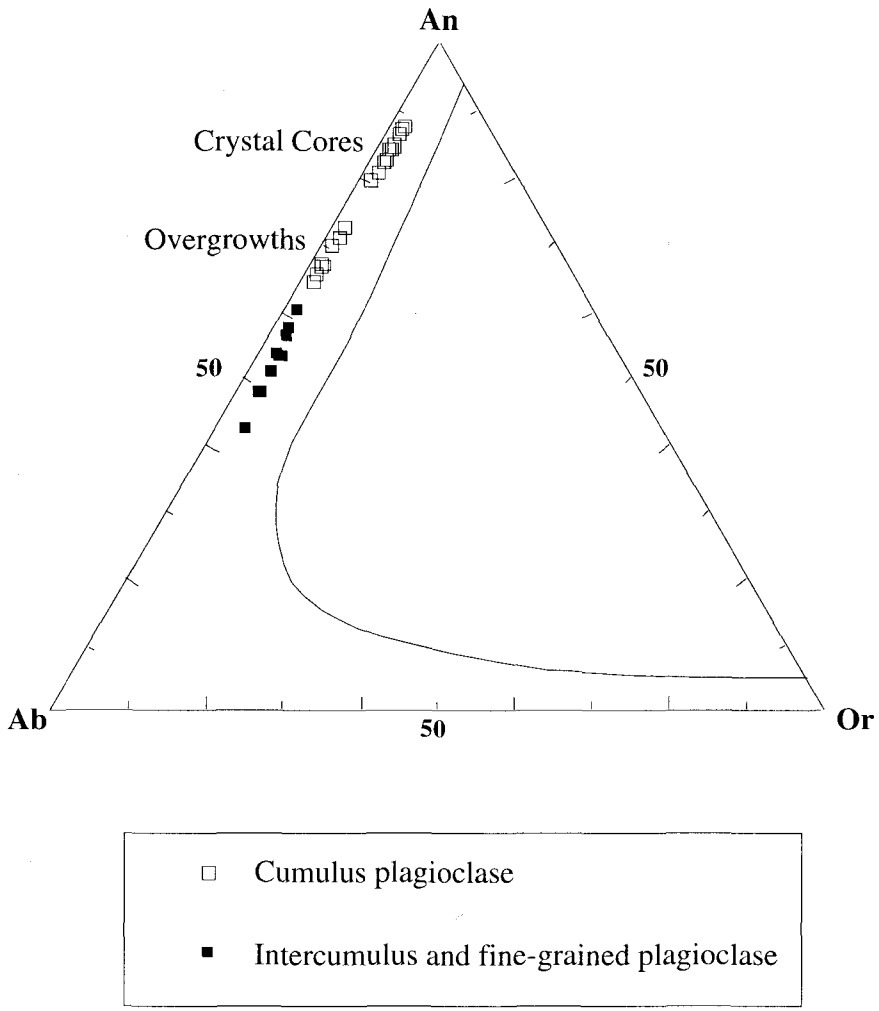

FIG. 9. Cumulus and intercumulus plagioclase compositions projected into the ternary Anorthite-Albite-Orthoclase at 2 kbar water pressure (after Tuttle and Bowen, 1958).

Plagioclase occurs in all of the ultramafic xenolith types, and is often a cumulus phase. Cumulus plagioclase is generally a highly calcic labradorite (An_{70}–An_{88}), and crystals show a range of zoning styles. The most common is that of an unzoned or slightly, normally zoned inner core making up the bulk of the crystal, with an outer rim showing strong, continuous normal zoning, especially where the crystal is in contact with fine-grained intercumulus material. Some crystals record evidence of a previous stage of resorption, having rounded cores, with euhedral overgrowths. Certain crystals exhibit well-developed oscillatory zoning, again with an unzoned or continuously zoned core, an oscillatory zoned outer section, and strongly normally zoned narrow overgrowths. Finally, some crystals display a patchily zoned core, often rich in inclusions of glass and other minerals, again with strongly normally zoned margins.

Zoning in igneous plagioclase is a very common phenomenon, and is controlled mainly by changes in the growth rate of individual crystals, and by the diffusion rate of ions at the crystal/liquid interface (Sibley *et al.*, 1976). Oscillatory zoning is thought to

TABLE 3. Representative electron probe micro-analyses of cumulus, intercumulus and fine-grained plagioclase from the ultramafic and gabbroic xenoliths

Sample	Feldspathic peridotite KBGX1		Pyroxenite KBGX2		Gabbro KBHYX1		Anorthosite KIFX1
Analysis no.	Cumulus	Fine grained	Inter-cumulus core	Inter-cumulus rim	Cumulus core	Cumulus rim	Cumulus core
SiO_2	44.77	53.31	53.38	57.83	46.36	49.84	46.68
TiO_2	0.00	0.05	0.06	0.07	0.03	0.00	0.09
Al_2O_3	35.32	29.35	28.20	25.36	34.01	31.74	33.27
FeO*	0.42	0.86	0.75	0.76	0.51	0.82	0.46
CaO	18.06	10.94	12.49	8.98	16.56	13.81	17.60
Na_2O	1.35	4.86	4.28	6.14	2.17	3.57	1.52
K_2O	0.03	0.31	0.21	0.61	0.06	0.14	0.10
Total	99.94	99.68	99.36	99.75	99.68	99.91	99.70
Formula on basis of 32 oxygens							
Si	8.28	9.70	9.76	10.44	8.57	9.12	8.63
Ti	0.00	0.01	0.01	0.01	0.00	0.00	0.01
Al	7.70	6.29	6.08	5.40	7.41	6.85	7.25
Fe (ii)	0.06	0.13	0.12	0.12	0.08	0.13	0.07
Ca	3.58	2.13	2.45	1.74	3.28	2.71	3.49
Na	0.48	1.72	1.52	2.15	0.78	1.27	0.55
K	0.01	0.07	0.05	0.14	0.01	0.03	0.02
Total	20.11	20.04	19.97	19.99	20.12	20.10	20.02
End-member %							
Ab	11.86	43.77	37.79	53.37	19.07	31.59	13.45
Or	0.17	1.84	1.24	3.48	0.34	0.79	0.55
An	87.97	54.39	60.97	43.15	80.59	67.62	85.99

result from the recurrent supersaturation of the melt in calcic plagioclase adjacent to individual crystals, possibly in response to shearing motions of the crystals within the magma (Vance, 1962; Anderson, 1984). The patchily-zoned, inclusion-rich, cores common in many igneous feldspars are thought to have crystallized in gas-saturated environments during periods of relatively high supersaturation in calcic plagioclase (Anderson, 1984).

Plagioclase crystals similarly zoned to those from the LSSC cumulates, have been described from the Skaergaard intrusion (Maaløe, 1976), and the Rum intrusion (Henderson and Suddaby, 1971; Young, 1984). Young (1984) suggested that complex zoning of some of the Rum plagioclase crystals was due to the penetration of newly emplaced primitive magma into the crystal mush on the intrusion floor. The presence of complex zoning in some of the plagioclases from the LSSC xenoliths is therefore consistent with the earlier proposed theory that the migration of melts through the crystal pile may have re-equilibrated cumulus olivine compositions in the peridotites.

Intercumulus plagioclases from the clinopyroxene-rich xenoliths are generally slightly less calcic ($An_{63}-An_{43}$) than the cumulus plagioclase in the peridotites, gabbros and anorthosite, and those from the intercumulus fine-grained areas of all xenolith types are typically strongly zoned from An_{57} to An_{45}, core to rim.

Spinel

Spinel occurs only within the olivine cumulates and is found as inclusions within cumulus olivines, in embayments in individual olivine crystals, and within intercumulus clinopyroxene and plagioclase. The spinel is considered to be an early cumulus phase. It is a chrome-spinel, with Cr contents varying between 33 and 42 wt.% Cr_2O_3. Individual crystals show no zoning, and no exsolution features are evident. Representative Cr-spinel analyses are documented in Table 4. Spinel compositions are also shown in Fig. 10*a*, projected on to the basal plane of the spinel prism, which illustrates the change in $Fe^{2+}/(Fe^{2+}+Mg)$ relative to Cr/(Cr+Al), and in Fig.

TABLE 4. Representative electron probe micro-analyses of cumulus Cr-spinel from the feldspathic peridotite xenoliths. All iron determined as FeO* and subsequently partitioned between ferrous and ferric iron by the method of Finger (1972)

Sample	Cumulus Cr-spinels trapped in cumulus olivine			Cumulus Cr-spinel trapped in intercumulus plagioclase and clinopyroxene			
Analysis No.	Cr-spinel 22	Cr-spinel 24	Cr-spinel 4	Cr-spinel 12	Cr-spinel 17	Cr-spinel 23	Cr-spinel 32
SiO_2	0.01	0.06	0.05	0.09	0.10	0.09	0.11
TiO_2	1.22	1.08	0.78	1.35	1.66	1.32	1.42
Al_2O_3	22.59	26.16	25.49	17.37	17.83	16.98	19.85
Cr_2O_3	36.71	33.20	34.34	42.00	40.78	42.26	39.29
Fe_2O_3	9.75	9.71	8.93	9.58	10.27	9.85	10.24
MgO	12.29	13.02	12.74	10.39	11.11	10.71	11.98
FeO	16.36	15.81	16.03	18.56	17.47	17.93	16.53
Total	98.94	99.04	98.35	99.34	99.23	99.14	99.42
Formula based on 32 oxygens							
Si	0.03	0.02	0.01	0.02	0.03	0.02	0.03
Ti	0.23	0.20	0.15	0.26	0.32	0.26	0.27
Al	6.63	7.53	7.40	5.26	5.36	5.15	5.88
Cr	7.23	6.41	6.69	8.53	8.23	8.60	7.81
Fe(iii)	1.83	1.79	1.66	1.85	1.97	1.91	1.94
Mg	4.53	4.74	4.68	3.98	4.23	4.11	4.49
Fe(ii)	3.41	3.23	3.30	3.99	3.73	3.86	3.48
Total	23.87	23.92	23.89	23.89	23.87	23.90	23.89
Fe/(Fe+Mg)	0.43	0.41	0.41	0.50	0.47	0.48	0.44
Cr/(Cr+Al)	0.52	0.46	0.48	0.62	0.61	0.63	0.57

10*b* which illustrates the variation of $Fe^{2+}/(Fe^{2+}+Mg)$ with $Fe^{3+}/(Fe^{3+}+Cr+Al)$. These diagrams show that the cumulus spinels found as inclusions in olivine crystals define a trend of increasing Cr/(Cr+Al) with little change in $Fe^{2+}/(Fe^{2+}+Mg)$. However, the spinels found dispersed through the intercumulus silicate phases (plagioclase and clinopyroxene) show a trend of increasing $Fe^{2+}/(Fe^{2+}+Mg)$ with little change in the Cr/(Cr+Al) ratio. Fig. 10*c* is a triangular plot of the trivalent cations in spinels (Cr^{3+}, Al^{3+}, Fe^{3+}). Crystals in the feldspathic peridotite xenoliths define a trend of increasing Al/Cr ratio with little change in Fe^{3+}. This trend has also been identified within spinels of the Eastern Layered Series of the Rum intrusion (Henderson, 1975; Henderson and Wood, 1981), from the Ben Buie layered gabbro, Isle of Mull (Henderson and Wood, 1981), and within the Cuillin Peridotite Series, Isle of Skye (Claydon, 1990; Bell and Claydon, 1992). These studies have recorded *two* divergent trends in Cr-spinel compositions. Henderson (1975) postulated that the 'Al-trend' documented above, was due to the reaction of the primary Cr-rich spinels with either olivine and plagioclase, or a melt rich in plagioclase components, making the spinels over to more Al-rich compositions. The 'Fe-trend' of more Fe^{3+}-rich spinels came about where the spinels were able to react with *trapped* intercumulus melt over a considerable temperature interval (Henderson, 1975; Henderson and Wood, 1981). The spinels found as inclusions in early formed cumulus olivine were thought to be the initial spinel which crystallized from the melt, and that their inclusion into early cumulus olivine prevented their reaction with the magma (Henderson, 1975). However, work by Scowen *et al.* (1991) has shown that olivine is very poor at retaining Cr-spinel compositions due to the ease with which cations can diffuse through the olivine structure. Those spinels completely encapsulated by plagioclase are more likely to maintain their magmatic compositions, since diffusion of cations through plagioclase in thought to be very difficult (Scowen *et al.*, 1991).

Within the peridotitic xenoliths, those spinels completely enclosed by cumulus olivine, have the highest Al and Mg contents (Fig. 10*d*), coupled with the lowest Ti concentrations. This is consistent with a high temperature, magmatic origin (*cf.* Henderson and Suddaby, 1971; Dunham and Wilkinson, 1985;

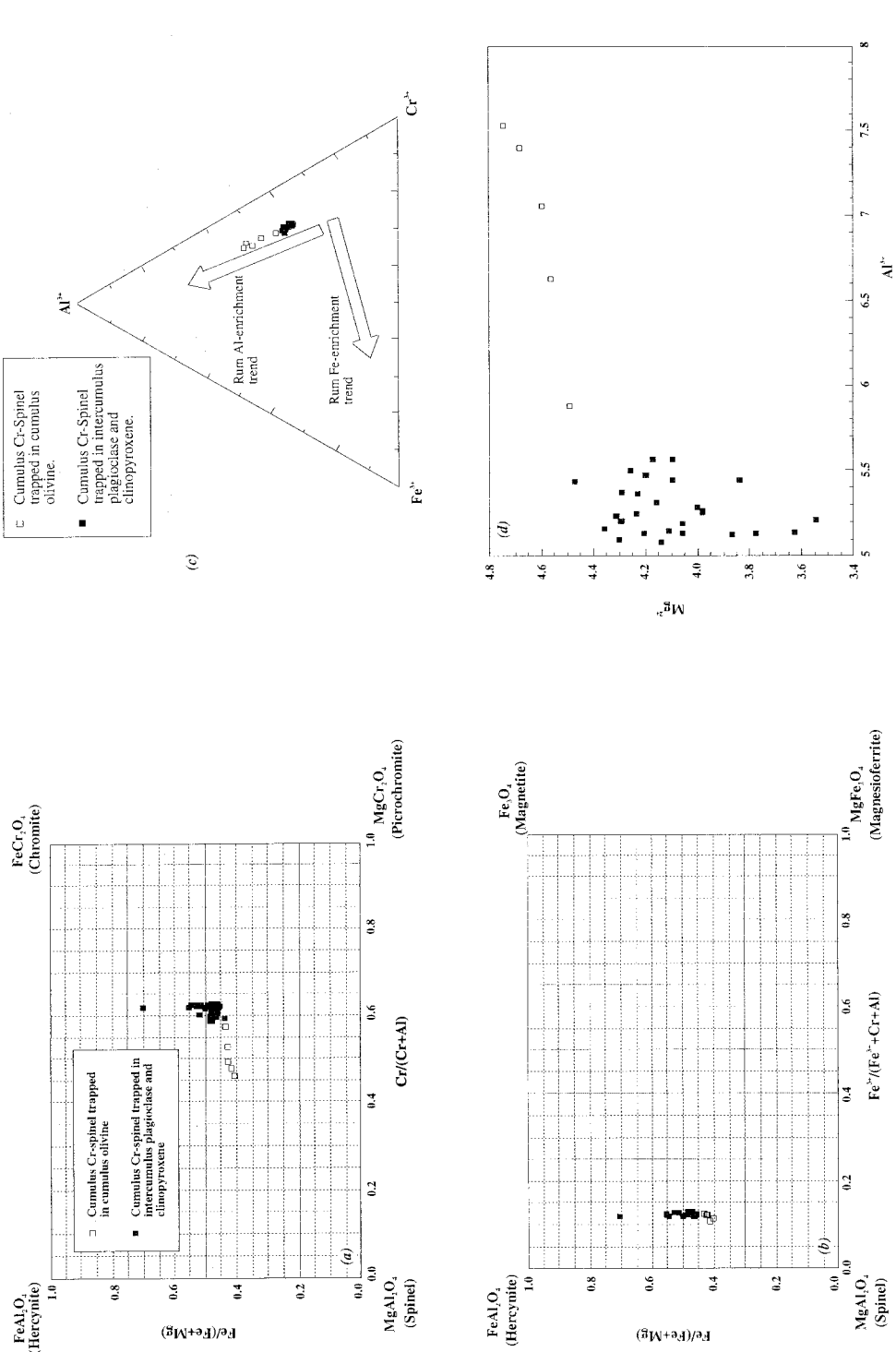

FIG. 10. Cr-spinel compositions projected onto (*a*) the base, and (*b*) the Fe-rich side, of the spinel prism; (*c*) variation in the trivalent cations of the Cr-spinels; (*d*) variation of cationic Al with Mg for the Cr-spinels.

Claydon, 1990). Those spinels found in embayments in cumulus olivine, and within intercumulus clinopyroxene and plagioclase, are enriched in Cr, Fe and Ti, relative to Mg and Al.

Experimental studies by Hill and Roeder (1974), and Fisk and Bence (1980) suggest that the chemistry of spinels crystallizing from basaltic liquids is controlled mainly by the temperature, pressure and oxygen fugacity (f_{O_2}) of the system. Hill and Roeder (1974) observed that with decreasing f_{O_2} the spinel crystallizes with increasing Mg/(Mg+Fe) and Al, and Fisk and Bence (1980) suggested that high-Al spinels crystallize at elevated pressures. However, many studies have emphasized the importance of post-cumulus and sub-solidus reactions and re-equilibration between spinels and silicate phases (Henderson and Suddaby, 1971; Henderson, 1975; Cameron, 1975; Roeder *et al.*, 1979; Henderson and Wood, 1981; Scowen *et al.*, 1991; Bell and Claydon, 1992).

The relationship between Cr-spinel composition and their textural position in the silicate phases of the peridotitic xenoliths suggest that the compositional variations are the result of post-cumulus reactions rather than an artefact of the crystallization history of the magma. It has been suggested, from similar relationships found in spinels from Rum and Muck basaltic lavas (Ridley, 1977), and in spinels from the Cuillin Peridotite Series (Bell and Claydon, 1992), that the initial Al-rich spinel reacts with the melt to give a more Cr-rich spinel, via a reaction such as:

Al-rich Cr-spinel + Melt →
Cr-rich Cr-spinel + Plagioclase

This is essentially the reverse of the reaction proposed by Henderson (1975) to account for the 'Al-trend' of the Rum peridotite spinels.

Ridley (1977) suggests that the interaction of early-formed Al-enriched spinel with a cooling silicate melt results from a peritectic reaction in which the spinel loses Al during the crystallization of plagioclase, with a concomitant increase in Fe and Ti. This is supported by the work of Dunham and Wilkinson (1985) who considered that the spinels became more Cr-enriched and Al-depleted after the onset of plagioclase crystallization.

The geothermometry equation of Fabriès (1979), based upon the mole fractions of Fe and Mg in coexisting olivines and spinels and the relative concentrations of the trivalent cations in the spinels, produces temperature estimates of between 1300°C and 800°C, with the Al- and Mg-rich spinels resulting in the highest temperatures. These temperatures are consistent with the hypothesis that it is the most Al- and Mg-rich, rather than the most Cr-rich spinels, which represent the first spinels to crystallize. However, it must be stressed that such empirical calibrations are subject to problems, especially when post-cumulus and subsolidus re-equilibration of both spinel and olivine are a major possibility (Roeder *et al.*, 1979; Fabriès, 1979; Bell and Claydon, 1992).

Whole-rock geochemistry

One sample of each xenolith type has been analysed for bulk-rock major-, trace- and rare-earth-element concentrations, and two samples for Sr and Nd isotope geochemistry. These data are given in Table 5; a typical composition of a host basaltic andesite is given for comparison. Since all the xenoliths are believed to be fragments of cumulate rocks, bulk-rock compositions are clearly controlled mainly by the relative proportions of olivine, plagioclase and pyroxene. For example, the olivine cumulate has high MgO and Ni contents, the xenoliths with cumulus plagioclase have high Sr values, and those rich in clinopyroxene have high V and Sc contents. The olivine-rich xenolith also has the highest Cr content (731 ppm), which is most likely due to the presence of minor Cr-spinel, and also the high Cr content of the intercumulus clinopyroxene of these early-formed cumulates. Later-formed, olivine-free cumulates have lower Cr contents, since the liquid would have been effectively depleted in Cr through the removal of early-precipitated Cr-spinel. The olivine-rich xenoliths have high LOI values (6.7 wt.%), indicating a high degree of alteration.

All xenolith types are depleted in the full range of incompatible elements when compared with the host rocks, again consistent with their cumulate origin. All xenolith types have flat to *LREE*-enriched rare-earth-element patterns, with the plagioclase cumulates having positive Eu anomalies (Fig. 11). Those xenoliths with abundant clinopyroxene typically have the highest total *REE* contents. However, the anorthosite shows the greatest *LREE* enrichment. Similar *LREE* enrichment in plagioclase has been found in anorthosites from the Eastern Layered Series of the Rum intrusion (Henderson and Gijbels, 1976; Palacz and Tait, 1985). The feldspathic peridotite has the lowest total *REE* content due to the dilution effect caused by the abundant olivine, which contains trivial amounts of *REE*.

The xenoliths have $^{87}Sr/^{86}Sr_{55}$ ratios of 0.708163 in the pyroxene cumulate, and 0.709226 in the anorthosite, and $^{143}Nd/^{144}Nd_{55}$ values of 0.511899 in the pyroxene cumulate, and 0.511929 in the anorthosite. Both initial Sr and Nd isotope ratios fall within the ranges of the host basalts and basaltic andesites (Fig. 12). The initial Sr ratios are more similar to the basalts of the LSSC rather than the more evolved rocks. Therefore, these less evolved specimens of the LSSC may still have been capable of precipitating ultrabasic cumulates. These data are

TABLE 5. Whole-rock major- and trace-element geochemistry and initial Sr-Nd isotope values from the four types of cumulate xenolith. Sr and Nd isotope ratios age-corrected to 55Ma (Bell and Jolley, in preparation)

	Feldspathic peridotite KBGX1	Pyroxenite KBGX2	Gabbro KBHYX1	Anorthosite KIFX1	Typical basaltic andesite
Major elements in wt.%					
SiO_2	42.50	51.50	50.82	46.20	54.06
TiO_2	0.27	0.58	0.40	0.13	1.62
Al_2O_3	8.24	10.50	16.31	30.26	14.29
Fe_2O_3*	11.05	7.84	5.58	2.17	11.62
MnO	0.17	0.15	0.10	0.02	0.18
MgO	26.88	11.05	8.06	0.77	5.06
CaO	3.81	14.54	14.79	13.95	8.39
Na_2O	0.51	1.94	1.97	2.34	2.91
K_2O	0.12	0.69	1.00	1.05	1.35
P_2O_5	0.02	0.04	0.03	0.02	0.14
LOI	6.73	1.17	1.08	2.67	0.75
Total	100.30	100.00	100.14	99.59	100.37
Trace elements in ppm					
Nb	1.3	1.3	1.2	1.4	7.4
Zr	26.0	47.5	32.3	25.9	145.4
Y	7.2	18.0	11.5	3.4	35.1
Sr	54.2	169.1	328.9	809.6	222.4
Rb	4.5	17.5	23.0	20.3	42.6
Th	0.2	0.0	0.0	0.0	7.4
Pb	0.0	3.4	4.1	6.3	8.1
Zn	75.5	70.2	45.1	27.7	104.0
Cu	13.1	36.8	17.0	59.9	32.3
Ni	805.9	72.4	22.3	84.9	14.3
Cr	731.1	273.6	171.6	24.7	42.8
V	86.6	273.0	189.1	30.8	209.0
Ba	42.8	530.7	693.6	784.8	455.0
Sc	19.8	78.9	50.7	5.4	43.2
La	3.03	5.46	3.75	3.50	19.32
Ce	6.82	12.41	8.09	8.86	44.04
Pr	0.75	1.51	0.95	1.05	5.01
Nd	3.08	7.35	4.78	3.27	19.30
Sm	0.81	1.73	1.13	0.67	4.31
Eu	0.32	0.68	0.50	0.57	1.28
Gd	0.99	2.37	1.54	0.74	4.96
Dy	1.00	2.47	1.58	0.58	4.95
Ho	0.24	0.57	0.35	0.14	1.15
Er	0.65	1.58	0.98	0.38	3.12
Yb	0.70	1.54	0.98	0.37	3.13
Lu	0.12	0.25	0.15	0.06	0.50
$^{87}Sr/^{86}Sr_i$		0.708163		0.709226	0.712282
$^{143}Nd/^{144}Nd_i$		0.511899		0.511929	0.511986

also consistent with crustal contamination of the basic magmas and their cumulates.

Preston (1996) has shown that the best-fit model for the evolution of the LSSC basic magmas is via a process of combined crustal assimilation and fractional crystallization (AFC; DePaolo, 1981), involving extensive interaction with metapelitic rocks of the Moine Group, or partial melts derived

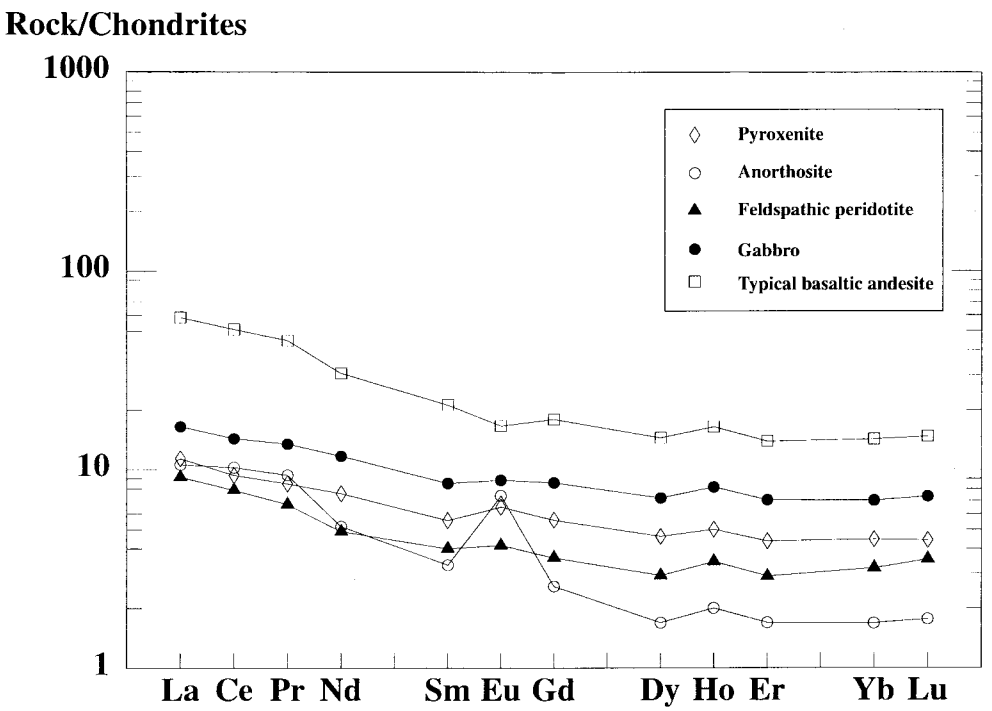

FIG. 11. Chondrite-normalized rare-earth-element plots for the various types of cognate xenolith, compared with a typical Group I basaltic andesite.

from them, at relatively high rates of assimilation. Initial Sr and Nd isotope ratios from two local Moine pelitic schists have the values $^{87}Sr/^{86}Sr_{55}$ = 0.7289–0.7299, and $^{143}Nd/^{144}Nd_{55}$ = 0.5118 (Preston, 1996). The slightly elevated $^{87}Sr/^{86}Sr_{55}$ ratios of the ultrabasic and gabbroic xenoliths, when compared with the least evolved host basalt, suggests that the some batches of the LSSC basic magma may have been extensively contaminated prior to the precipitation of the cumulates. The initial Nd isotope values of both the cumulates and the majority of the basic sills scatter around 0.5119 to 0.5120, again implying that contamination of the basic magmas occurred relatively early in their evolution, and that Nd isotopic values were buffered by the Nd isotope values of the contaminants.

These data suggest that a process similar to that proposed by Reiners *et al.* (1995, 1996) may have been in operation within the LSSC magma processing reservoir(s). Their work on ultramafic-granitic composite plutons in Alaska, showed that some of the early formed ultramafic cumulate rocks have enriched isotopic signatures. Without firm evidence of an enriched mantle source for the parent magmas to these cumulates, Reiners *et al.* (1996) suggest that the isotopic characteristics were the result of crustal contamination. Van der Laan and Wyllie (1993) have shown that the interaction of mafic melts with silicic melts rich in alkalis and H_2O results in the lowering of the liquidus temperature of the melt, and Sisson and Grove (1993) suggest that this process will also enlarge the stability field of olivine at the expense of plagioclase and clinopyroxene. In this way, the early stages of AFC are characterised by high rates of assimilation, without much crystallization (perhaps olivine alone). This results in large shifts in the isotopic and trace-element characteristics of the magmas with little major-element differentiation. The second stage of AFC, beginning with the crystallization of plagioclase and pyroxene, is characterized by lower rates of assimilation, and the magma evolves more rapidly (Reiners *et al.*, 1995).

Within the LSSC, the rhyolitic members of the suite are derived predominantly through partial melting of the Moine metasediments, as shown by their very high initial Sr isotope ratios (up to 0.7203). Highly silicic melts are also preserved in some of the crustal xenoliths (Preston, 1996). Given the

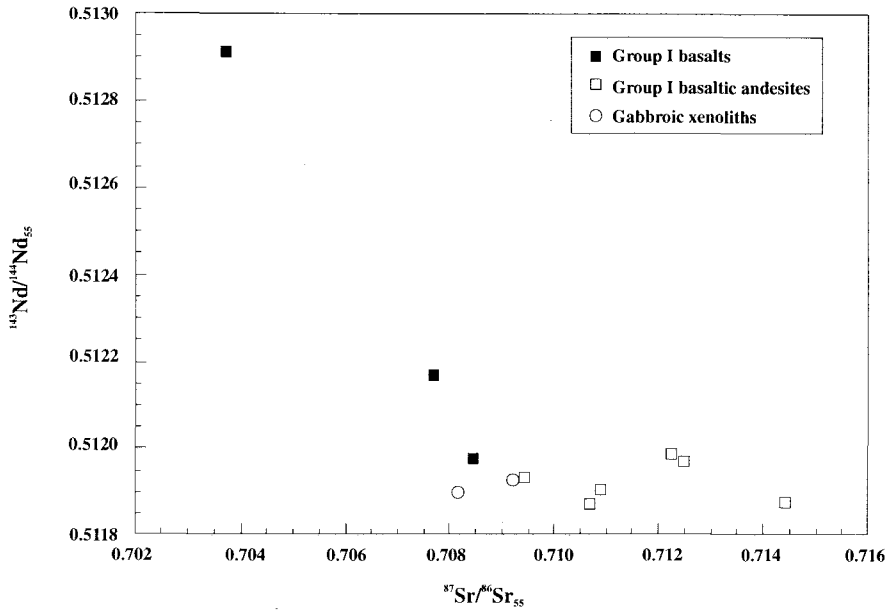

FIG 12. $^{143}Nd/^{144}Nd_{55}$ *vs.* $^{87}Sr/^{87}Sr_{55}$ for the cognate xenoliths compared to their host basaltic Group I sheets. Data for Group I basalts and basaltic andesites from Preston (1996).

combined data on the sheets, and the gabbroic and crustal xenoliths, it is suggested therefore, that the mode of contamination of the basic magmas may have been through interaction with alkali- and H_2O-enriched felsic melts derived from the metamorphic basement rocks.

Origin and significance of the gabbroic xenoliths

The lack of a high-pressure mineral assemblage (for example, no chrome-diopside or garnet), and the cumulate textures of these xenoliths, precludes them from representing fragments of mantle material. The host sheets were intruded through Neoproterozoic basement rocks, Mesozoic sedimentary rocks and Palaeogene lavas. As a result it is possible that the gabbroic xenoliths represent accidental inclusions ripped-up from a pre-existing gabbroic body formed from the crystallization of the magmas which formed the plateau lavas. However, the Palaeogene lava field is composed in the main of transitional to mildly alkaline olivine basalts and their differentiates (the so-called Mull Plateau Group; Kerr, 1995). A small number of thick tholeiitic flows occur locally at the base of the succession (the Staffa Magma Type; Thompson *et al.*, 1986). The highly calcic nature of the cumulus plagioclase, and the low Al, Ti and Na contents of the clinopyroxenes suggests that the xenoliths crystallized from a tholeiitic magma (*cf.* pyroxene analyses in Thompson, 1974). The pyroxenes are also all hypersthene normative, and define an iron-enrichment trend identical to those from the Skaergaard intrusion (Brown, 1957), substantiating the requirement for a tholeiitic parent magma. Since there is no geophysical evidence for an extensive sub-surface gabbroic body in the Loch Scridain region (Bott and Tantrigoda, 1987), it is therefore considered most likely that the xenoliths are indeed cognate to the LSSC magmas, and represent early-formed precipitates. Although the possibility that the xenoliths are crystal-enriched differentiates from the Staffa Magma type lavas cannot be discounted, it seems more likely that such material would have been cleared from the system by the passage of the large amounts of alkaline magma which make up the bulk of the lava field. The fact that phenocrysts and glomeroporphyritic clots of the same mineralogy as the larger xenoliths also occur in the LSSC magmas also provides strong evidence for a cognate origin for the xenoliths, as does the similarity in initial Sr and Nd isotopic values between the gabbroic xenoliths and the more basic members of the LSSC.

The occurrence of gabbroic xenoliths within members of the LSSC, provides perhaps some of the best evidence that fractional crystallization of the parent magmas was occurring within the Loch Scridain magma chamber(s). The xenoliths provide some evidence as to the early evolution of the Loch

Scridain magmas, with knowledge of mineral and bulk-rock compositions enabling a few constraints to be put on the nature of the parent magma(s) of the LSSC.

The presence of near-monomineralic xenoliths with markedly different major cumulus phases (olivine, plagioclase, or clinopyroxene) suggests that a magma chamber, similar to those now represented by the Rum and Skye ultrabasic layered intrusions, was involved in the formation of the LSSC. The parent magma(s) for these intrusions has been argued to be basaltic (Brown, 1956), picritic (Huppert and Sparks, 1980), and eucritic with suspended olivine crystals (Gibb, 1976). Kitchen (1985) suggested that the parental magma for the Rum intrusion was more alkaline in nature, rather than tholeiitic, on the evidence of alkaline segregation veins found within some of the peridotites.

Within layered intrusions, the presence of near monomineralic cumulates has provided petrologists with a subject for debate for many years. Numerous hypotheses have been suggested to explain features such as cyclical layering, cryptic layering and rhythmic layering (Irvine, 1987). Huppert and Sparks (1980) provide a general model for the development of igneous layering which has been applied to explain the formation of the cyclical ultrabasic units of the Rum intrusion (Palacz and Tait, 1985; Emeleus, 1987). Their model suggests that the magma chamber undergoes repeated replenishments with batches of picritic magma which pond at the base of the chamber underneath lighter, cooler and more-evolved residual magma from previous events. Initial abundant olivine crystallization lowers the density of the picritic magma, which then cools against the overlying magma, causing strong convection within the picritic magma. This process forms the peridotitic layers. Once the two magmas have achieved approximately the same densities and temperature, the boundary between them breaks down, plagioclase joins olivine as a liquidus phase, leading to the formation of the troctolitic (plagioclase-olivine) layers. Crystallization of olivine, plagioclase and minor clinopyroxene will continue forming thick troctolitic layers until a new influx of picritic magma ejects the resident evolved magma and restarts the cycle. Although it is obviously impossible to confirm whether such a mechanism occurred during the crystallization of the LSSC magmas, the enrichment of relatively-evolved LSSC magmas in Cr and Ni suggests that the evolution of the basic magmas probably involved replenishment events. Such a process can therefore account for the olivine-rich and gabbroic xenoliths. However the presence of near-monomineralic pyroxenites and anorthosites requires that a mechanical crystal separating process was also operating. Although it is impossible to tell the nature of this process from the evidence provided by the cognate xenoliths, factors such as gravity settling of pyroxene, floatation of plagioclase, or filter pressing may have been important.

The cumulus phases found in the Loch Scridain xenoliths are similar in composition to those found in both the Rum and Skye ultrabasic rocks, although the olivines do not extend to such high Fo contents, and the cumulus plagioclases are generally less calcic (Faithfull, 1985; Tait, 1985; Palacz and Tait, 1985; Claydon and Bell, 1992). Olivine of composition Fo_{85}, typical of that found in the olivine-bearing xenoliths, would be in equilibrium with a basic liquid with 9-10 wt.% MgO (Roeder and Emslie, 1970). This composition is basaltic rather than picritic or ultrabasic, although there is some evidence that olivine compositions are easily re-equilibrated through post-cumulus processes (Faithfull, 1985; Tait, 1985; Palacz and Tait. 1985; Claydon and Bell, 1992).

Bulk-rock Cr and Ni contents of the olivine and pyroxene cumulates are also more consistent with a basaltic parent; Cr contents reach over 6000ppm, and Ni over 1900ppm, in some of the Rum peridotites (Tait, 1985). The abundant cumulus clinopyroxene also points to a basaltic parent magma (Gibb, 1976; Claydon and Bell, 1992).

Within the BTIP, three distinct magma types are recognised (Thompson *et al.*, 1972, 1980; Mattey *et al.*, 1977): the so-called Skye Main Lava Series (SMLS), the tholeiitic Fairy Bridge (FB) magma type, and the MORB-like tholeiitic Preshal More (PM) magma type. The major geochemical characteristics of these three magma types have been summarised by Bell *et al.* (1994). These are equivalent to the three magma types recently re-evaluated from the Mull lava pile, with the Mull Plateau Group, the Coire Gorm magma type, and the Central Mull Tholeiites corresponding to the SMLS, FB and PM magma types, respectively (Kerr, 1995).

Preston (1996) has shown that the parent magmas to the LSSC were most likely of the PM magma type. The cumulate xenoliths fit in with this hypothesis, in that they crystallized from a tholeiitic magma, and have incompatible trace-element characteristics which generally fall well within the range shown by PM magmas (e.g. $Y/Zr > 0.3$). The one exception to this is the anorthosite. However, the distinct lack of intercumulus material in this rock, which may have been removed via a filter-pressing action, would explain why its trace-element characteristics are anomalous.

The Sr-Nd isotope data show that the magmas were contaminated with crustal material derived from the pelitic schists of the Moine crystalline basement during fractionation. The fact that the cumulates are

also slightly contaminated compared to the least-evolved host basalt, suggests that the parent magmas may actually have ponded and fractionated within the Moine lithologies, rather than being contaminated during their passage through the crust (*cf.* Kerr *et al.*, 1995).

The presence of cognate cumulates within a suite of essentially aphyric sheets enables some constraints to be placed upon the temperature of crystallization of the early-formed products. Application of the Kudo-Weill plagioclase thermometer (Kudo and Weill, 1970; Mathez, 1973), yields dry, liquidus temperatures of between 1300°C for cumulus plagioclase from the feldspathic peridotites, and 1250°C for cumulus plagioclase from the gabbros. Temperatures for cumulus clinopyroxene, using the method of Kretz (1982), vary from 1250°C (gabbros) to 1000°C (pyroxenites). These temperatures are generally consistent with down-temperature crystallization of olivine, followed by plagioclase, then clinopyroxene, from a tholeiitic basalt magma. However, it must be stressed that, as with the Cr-spinel geothemometry, the lower temperatures may be recording sub-solidus re-equilibration events. The presence of abundant cumulus plagioclase also suggests that the magma storage reservoirs to the LSSC were at relatively shallow crustal levels (Green and Ringwood, 1967). Indeed, the phase relationships of the basic host magmas shows that they were probably in pre-emplacement cotectic equilibrium at approximately 2–3 kbar (Preston, 1996). This pattern of low-pressure coupled fractionation and assimilation of Preshal More type tholeiitic magmas is repeated elsewhere in the BTIP (e.g. the Skye cone sheets, Bell *et al.*, 1994), and contrasts with the majority of the Mull and Skye lavas, which exhibit elemental and isotopic evidence for lower-crustal contamination after crystal-liquid fractionation (Thirlwall and Jones, 1983; Dickin *et al.*, 1987).

Summary

The xenoliths preserved in the Loch Scridain Sill Complex consist of feldspathic peridotite, gabbro, clinopyroxenite and anorthosite. All of the xenoliths have low pressure mineralogies and cumulate textures, and therefore cannot represent fragments of the upper mantle beneath Mull, but rather represent early-formed precipitates, cognate to the host sheets. Mineralogical and trace-element data suggest that the parent magma to the xenoliths was a tholeiitic basalt similar to the MORB-like Preshal More magma type. Initial Sr and Nd isotope ratios for two of the xenoliths show that they are slightly contaminated with crustal material. The Sr-Nd isotope values fall within the range of some of the least-evolved host magmas, suggesting that contamination of the cumulates occurred at a relatively early stage. It is suggested that magma replenishment events within the LSSC magma storage reservoirs may have controlled the near-monomineralic nature of certain of the cumulate xenoliths. These xenoliths also provide direct evidence for the process of combined assimilation and fractional crystallization within sub-volcanic conduits, and provide another rare example of this process occurring within the British Tertiary Igneous Province.

Acknowledgements

Thanks go to Graeme Rogers and Malcolm Hole for helpful and constructive comments on a earlier draft of this paper. Colin Donaldson and an anonymous reviewer provided invaluable criticisms of the manuscript. We are most grateful to Godfrey Fitton and Doddie James, Department of Geology and Geophysics, University of Edinburgh, for provision of major- and trace-element data. Nick Walsh of Royal Holloway University, London, kindly made available analytical facilities for the *REE*. Robert MacDonald provided the technical assistance for the electron probe analysis at the Department of Geology and Applied Geology, University of Glasgow. Anne Kelly and Vincent Gallagher are thanked for their sterling efforts in the radiogenic isotope laboratories at the SURRC. R.J.Preston acknowledges with gratitude the receipt of a NERC training award (1992-1995). The isotopic analyses at SURRC were supported by the Scottish Universities.

References

Anderson, A.T.J. (1984) Probable relations between plagioclase zoning and magma dynamics, Fuego Volcano, Guatemala. *Amer. Mineral.*, **69**, 660–76.

Arculus, R.J. and Wills, K.J.A. (1980) The petrology of plutonic blocks and inclusions from the Lesser Antillies island arc. *J. Petrol.*, **21**, 743–99.

Bailey, E.B., Clough, C.T., Wright, W.B., Richey, J.E. and Wilson, G.V. (1924) Tertiary and Post-Tertiary geology of Mull, Loch Aline, and Oban. *Mem. Geol. Surv. Scotland.* H.M.S.O., Edinburgh.

Barbero, L., Villaseca, C., Rogers, G. and Brown, P.E. (1995) Geochemical and isotopic disequilibrium in crustal melting: an insight from the anatectic granitoids from Toledo, Spain. *J. Geophys. Res.*, **100(B8)**, 15745–65.

Bell, B.R. and Claydon, R.V. (1992) The cumulus and post-cumulus evolution of chrome-spinels in ultra-basic intrusions: Evidence from the Cuillin Igneous Complex, Isle of Skye, Scotland. *Contrib. Mineral. Petrol.*, **112**, 242–53.

Bell, B.R., Claydon, R.V. and Rogers, G. (1994) The petrology and geochemistry of cone-sheets from the

Cuillin Igneous Complex, Isle of Skye: Evidence for combined assimilation and fractional crystallization during lithospheric extension. *J. Petrol.* **35**, 1055–94.

Binns, R. A. (1969) High-pressure megacrysts in basaltic lavas near Armidale, New South Wales. *Amer. J. Sci.*, **267-A**, 33–49.

Binns, R.A., Duggan, M.B. and Wilkinson, J.F.G. (1970) High pressure megacrysts in alkaline lavas from north-eastern New South Wales. *Amer. J. Sci.*, **269**, 132–68.

Bott, M.H.P. and Tandrigoda, T.A. (1987) Interpretation of the gravity and magnetic anomalies over the Mull Tertiary intrusive complex, NW Scotland. *J. Geol. Soc., London,* **91,** 17–28.

Brown, G.M. (1956) The layered ultrabasic rocks of Rhum, Inner Hebrides. *Phil. Trans. Roy. Soc. London,* **B240**, 1–53.

Brown, G.M. (1957) Pyroxenes from the early and middle stages of fractionation of the Skaergaard intrusion, East Greenland. *Mineral. Mag.*, **31**, 511–43.

Brown, G.M. and Vincent, E.A. (1963) Pyroxenes from the late stages of fractionation of the Skaergaard intrusion, East Greenland. *J. Petrol.*, **4**, 175–97.

Cameron, E.N. (1975) Postcumulus and subsolidus equilibration of chromite and coexisting silicates in the Eastern Bushveld Complex. *Geochim. Cosmochim. Acta,* **39**, 1021–33.

Cigolini, C. and Kudo, A.M. (1987) Xenoliths in recent basaltic andesite flows from Arenal Volcano, Costa Rica: Inference on the composition of the lower crust. *Contrib. Mineral. Petrol.*, **96**, 381–90.

Claydon, R.V. (1990) *A petrological study of mafic hypabyssal and ultramafic plutonic rocks of the Cuillin Igneous Complex, Isle of Skye, Scotland.* Unpublished PhD thesis, University of Glasgow.

Claydon, R.V. and Bell, B.R. (1992) The structure and petrology of ultrabasic rocks in the southern part of the Cuillin Igneous Complex, Isle of Skye. *Trans. Roy. Soc. Edinburgh,* **83**, 635–53.

Conrad, W.K. and Kay, R.W. (1984) Ultramafic and mafic inclusions from Adak Island: Crystallization history, and implications for the nature of primary magmas and crustal evolution in the Aleutian Arc. *J. Petrol.*, **25**, 88–125.

DeLong, S.E., Hodges, F.N. and Arculus, R.J. (1975) Ultramafic and mafic inclusions, Kanga Island, Alaska, and the occurrence of alkaline rocks in island arcs. *J. Geol.*, **83**, 721–36.

DePaolo, D.J. (1981) Trace element and isotopic effects of combined wallrock assimilation and fractional crystallization. *Earth Planet. Sci. Lett.*, **53**, 189–202.

Dickin, A.P., Jones, N.W., Thirlwall, M.F. and Thompson, R.N. (1987) A Ce/Nd isotope study of crustal contamination processes affecting Palaeocene magmas in Skye, Northwest Scotland. *Contrib. Mineral. Petrol.*, **96**, 455–64.

Donaldson, C.H. (1977) Petrology of anorthite-bearing gabbroic anorthosite dykes in north-west Skye. *J. Petrol.*, **18**, 595–620.

Duke, J.M. (1976) Distribution of the period four transition elements among olivine, calcic clinopyroxene and mafic silicate liquids: Experimental results. *J. Petrol.*, **17**, 499–521.

Dunham, A.C. and Wilkinson, F.C.F. (1985) Sulphide droplets and the Unit 11/12 chromite band, Rhum: A mineralogical study. *Geol. Mag.*, **122**, 539–48.

Emeleus, C.H. (1987) The Rhum layered complex, Inner Hebrides, Scotland. In: Parsons, I. (ed.) *Origins of Igneous Layering*, Reidel Publishing, Dortrecht, 263–86.

Esson, J., Dunham, A.C. and Thompson, R.N. (1975) Low alkali, high calcium olivine tholeiite lavas from the Isle of Skye, Scotland. *J. Petrol.*, **16**, 488–97.

Evans, B.W. and Moore, J.G. (1968) Mineralogy as a function of depth in the pre-historic Makaopuhi tholeiitic lava lake, Hawaii. *Contrib. Mineral. Petrol.*, **17**, 85–115.

Fabriès, J. (1979) Spinel-olivine geothermometry in peridotites from ultrabasic complexes. *Contrib. Mineral. Petrol.*, **69**, 329–36.

Faithfull, J.W. (1985) The Lower Eastern Layered Series of Rhum. *Geol. Mag.*, **122**, 459–68.

Finger, L.W. (1972) The uncertainty in the calculated ferric iron content of a microprobe analysis. *Carnegie Institute Washington Yearbook*, **71**, 600–603.

Fisk, M.R. and Bence, A.E. (1980) Experimental crystallization of chrome spinel in FAMOUS basalt 567-1-1. *Earth Planet. Sci. Lett.*, **48**, 111–23.

Fitton, J.G. and Dunlop, H.M. (1985) The Cameroon line, West Africa, and its bearing on the origin of oceanic and continental alkali basalt. *Earth Planet. Sci. Lett.*, **72**, 23–38.

Gibb, F.G.F. (1969) Cognate xenoliths in the Tertiary ultrabasic dykes of south-west Skye. *Mineral. Mag.*, **37**, 504–14.

Gibb, F.G.F. (1973). The zoned clinopyroxenes of the Shiant Isles sill, Scotland. *J. Petrol.*, **14**, 203–30.

Gibb, F.G.F. (1976) Ultrabasic rocks of Rhum and Skye: The nature of the parent magma. *J. Geol. Soc., London,* **132**, 209–22.

Green. D.H. and Ringwood, A.E. (1967) The genesis of basaltic magmas. *Contrib. Mineral. and Petrol.*, **15**, 103–90.

Harris, C. (1983) The petrology of lavas and associated plutonic inclusions of Ascension Island. *J. Petrol.*, **24**, 424–70.

Henderson, P. (1975) Reaction trends shown by chrome-spinels of the Rhum layered intrusion. *Geochim. Cosmochim. Acta,* **39**, 1035–44.

Henderson, P. and Gijbels, R. (1976) Trace element indicators of the genesis of the Rhum layered

intrusion, Inner Hebrides. *Scottish J. Geol.*, **12**, 325–33.

Henderson, P. and Suddaby, P. (1971) The nature and origin of the chrome-spinel of the Rhum layered intrusion. *Contrib. Mineral. Petrol.*, **33**, 21–31.

Henderson, P. and Wood, R.J. (1981) Reaction relationships of chrome-spinels in igneous rocks — Further evidence from the layered intrusions of Rhum and Mull, Inner Hebrides, Scotland. *Contrib. Mineral. Petrol.*, **78**, 225–9.

Hill, R. and Roeder, P. (1974) The crystallization of spinel from basaltic liquid as a function of oxygen fugacity. *J. Geol.*, **82**, 709–29.

Huppert, H.E. and Sparks, R.S.J. (1980) The fluid dynamics of a basaltic magma chamber replenished by an influx of hot dense ultrabasic liquid. *Contrib. Mineral. Petrol.*, **75**, 279–89.

Irvine, T.N. (1987) Processes involved in the formation and development of layered igneous rocks. In: Parsons, I. (ed) *Origins of Igneous Layering*. Reidel, Dortrecht, 649–56.

Janošek, V., Rogers, G. and Bowes, D.R. (1995) Sr-Nd isotopic constraints on the petrogenesis of the Central Bohemian Pluton, Czech Republic. *Geol. Rundsch.*, **84**, 520–34.

Kerr, A.C. (1995) The geochemistry of the Mull-Morvern Tertiary lava succession, NW Scotland: An assessment of mantle sources during plume-related volcanism. *Chem. Geol.*, **122**, 43–58.

Kerr, A.C., Kempton, P.D. and Thompson, R.N. (1995) Crustal assimilation during turbulent magma ascent (ATA); new isotopic evidence from the Mull Tertiary lava succession, N.W. Scotland. *Contrib. Mineral. Petrol.*, **119**, 142–54.

Kitchen, D.E. (1985) The parental magma on Rhum: Evidence from alkaline segregations and veins in the peridotites from Salisbury's Dam. *Geol. Mag.*, **122**, 529–37.

Kretz, R. (1982) Transfer and exchange equilibria in a portion of the pyroxene quadrilateral as deduced from natural and experimental data. *Geochimic. Cosmochim. Acta*, **46**, 411–21.

Kudo, A.M. and Weill, D. (1970) An igneous plagioclase geothermometer. *Contrib. Mineral. Petrol.*, **25**, 52–65.

Maaløe, S. (1976) The zoned plagioclase of the Skaergaard intrusion, East Greenland. *J. Petrol.*, **17**, 398–419.

Mathez, E.A. (1973) Refinement of the Kudo-Weill plagioclase geothermometer and its application to basaltic rocks. *Contrib. Mineral. Petrol.*, **41**, 61–72.

Mattey, D.P., Gibson, I.L., Marriner, G.F. and Thompson, R.N. (1977) The diagnostic geochemistry, relative abundance, and spatial distribution of high-calcium, low-alkali olivine tholeiite dykes in the Lower Tertiary regional swarm of the Isle of Skye, NW Scotland. *Mineral. Mag.*, **41**, 273–85.

McBirney, A.R. and Hunter, R.H. (1995) The cumulate paradigm reconsidered. *J. Geol.*, **103**, 114–22.

Munha, J., Palacios, T., MacRae, N.D. and Mata, J. (1990) Petrology of ultramafic xenoliths from Madeira island. *Geol. Mag.*, **127**, 543–66.

Palacz, Z.A. and Tait, S.R. (1985) Isotopic and geochemical investigation of Unit 10 from the Eastern Layered Series of the Rhum Intrusion, Northwest Scotland. *Geol. Mag.*, **122**, 485–90.

Preston, R.J. (1996) *The petrogenesis of the Loch Scridain Xenolithic Sill Complex, Isle of Mull*. Unpublished PhD thesis, University of Glasgow.

Reiners, P.W., Nelson, B.K. and Ghiorso, M.S. (1995) Assimilation of felsic crust by basaltic magma: Thermal limits and extents of crustal contamination of mantle-derived magmas. *Geology*, **23**, 563–6.

Reiners, P.W., Nelson, B.K. and Nelson, S.W. (1996) Evidence for multiple mechanisms of crustal contamination of magma from compositionally zoned plutons and associated ultramafic intrusions of the Alaska Range. *J. Petrol.*, **37**, 261–92.

Ridley, W.I. (1977) The crystallization trends of spinels in Tertiary basalts from Rhum and Muck and their petrogenetic significance. *Contrib. Mineral. Petrol.*, **64**, 243–55.

Roeder, P.L. and Emslie, R.F. (1970) Olivine-liquid equilibrium. *Contrib. Mineral.Petrol.*, **29**, 275–89.

Roeder, P.L., Campbell, I.H. and Jamieson, H.E. (1979) A re-evaluation of the olivine-spinel geothermometer. *Contrib. Mineral. Petrol.*, **68**, 325–34.

Scowen, P.A.H., Roeder, P.L. and Helz, R.T. (1991) Re-equilibration of chromite within Kilauea Iki lava lake, Hawaii. *Contrib. Mineral. Petrol.*, **107**, 8–20.

Sibley, D.F., Vogel, T.A., Walker, B.M. and Byerly, G. (1976) The origin of oscillatory zoning in plagioclase: A diffusion and growth controlled model. *Amer. J. Sci.*, **276**, 275–84.

Sisson, T.W. and Grove, T.L. (1993) Experimental investigations of the role of H_2O in calc-alkaline differentiation and subduction zone magmatism. *Contrib. Mineral. Petrol.*, **113**, 143–66.

Tait, S.R. (1985) Fluid dynamic and geochemical evolution of cyclic Unit 10, Rhum, Eastern Layered Series. *Geol. Mag.*, **122**, 469–84.

Thirlwall, M.F. and Jones, N.W. (1983) Isotope geochemistry and contamination mechanics of Tertiary lavas from Skye, Northwest Scotland. In: Hawkesworth, C.J. and Norry, M.J. (eds.) *Continental Basalts and Mantle Xenoliths*. Shiva Publishing, Cheshire, 186–250.

Thompson, R.N. (1974) Primary basalts and magma genesis. I. Skye, North west Scotland. *Contrib. Mineral. Petrol.*, **45**, 317–41.

Thompson, R.N., Esson, J. and Dunham, A.C. (1972) Major element chemical variation in the Eocene lavas of the Isle of Skye, Scotland. *J. Petrol.*, **13**, 219–53.

Thompson, R.N., Gibson, I.L., Marriner, G.F., Mattey, D.P. and Morrison, M.A. (1980) Trace-element evidence of multistage mantle fusion and polybaric fractional crystallization in the Palaeocene lavas of Skye, NW Scotland. *J. Petrol.*, **21**, 265–93.

Thompson, R.N., Morrison, M.A., Dickin, A.P., Gibson, I.L. and Harmon, R.S. (1986) Two contrasting styles of interaction between basic magmas and continental crust in the British Tertiary Volcanic Province. *J. Geophys. Res.*, **91(B6)**, 5985–97.

Tuttle, O.F. and Bowen, N.L. (1958). Origin of granite in the light of experimental studies in the system $NaAlSi_3O_8$-$KAlSi_3O_8$-SiO_2-H_2O. *Geol. Soc. Amer. Memoirs*, **74**, 153pp.

Vance, J.A. (1962) Zoning in igneous plagioclase: Normal and oscillatory zoning. *Amer. J. Sci.*, **260**, 746–60.

Van der Laan, S.R. and Wyllie, P.J. (1993) Experimental interaction of granitic and basaltic magmas and implications for mafic enclaves. *J. Petrol.*, **34**, 491–517.

Wager, L.R., and Brown, G.M. (1968) *Layered Igneous Rocks*. Oliver and Boyd, Edinburgh and London, 588 pp.

Wager, L.R., Brown, G.M. and Wadsworth, W.J. (1960) Types of igneous cumulate. *J. Petrol.*, **1**, 73–85.

Walsh, J.N., Buckley, F. and Barker, J. (1981) The simultaneous determination of the rare earth elements in rocks using inductively coupled plasma source spectrometry. *Chem. Geol.*, **33**, 141–53.

Young, I.M. (1984) Mixing of supernatant and intercumulus fluids in the Rhum layered intrusion. *Mineral. Mag.*, **48**, 345–50.

[*Manuscript received 28 August 1996: revised 25 November 1996*]